Bull. Mater. Sci., Vol. 40, No. 6, October 2017, pp. 1069–1074
DOI 10.1007/s12034-017-1465-2

Hydrothermal growth of wheatear-shaped ZnO microstructures and their photocatalytic activity

PING LI[1,*], BIN LU[1] and ZHANZHOU LUO[2]
[1]School of Chemistry and Materials Science, Hebei Normal University, Shijiazhuang 050024, China
[2]School of Chemical and Material Engineering, Jiangnan University, Wuxi 214122, China
*Author for correspondence (liping@hebtu.edu.cn)

MS received 29 August 2016; accepted 6 February 2017; published online 12 September 2017

Abstract. A facile hydrothermal process was developed to synthesize novel wheatear-shaped ZnO microstructures at a low temperature (85°C) without the assistance of any template agent. X-ray diffraction and field emission scanning electron microscopy were used to characterize the structure and morphology of the samples. Results showed that the length of the 'wheatear' was about 5.8 μm and the section width was 1.2 μm. The particles consisted of closely packed nanorods with average diameter of 100 nm. The growth of wheatear-shaped ZnO is very rapid and can be achieved in only 5 min. OH^--driven oriented aggregation and multistep nucleation resulted in the formation of wheatear-shaped ZnO microstructures. The product had assembled open structures and it exhibited excellent photocatalytic activity in the degradation of methyl orange under UV-light irradiation.

Keywords. Wheatear-shaped ZnO; hydrothermal synthesis; rapid growth; photocatalytic properties.

1. Introduction

ZnO is an important semiconductor material with a wide band gap of 3.37 eV and a large exciton binding energy of 60 meV [1]. Due to its excellent performance, it has been extensively used in optoelectronics, solar cells, sensors, photocatalysts, piezoelectric devices, light-emitting devices and biomedical applications [2–6]. Recently, ZnO with complex hierarchical structures has attracted considerable attention because of its unique properties, which differ considerably from the mono-morphological ones [7–10]. It has been reported that hierarchical ZnO structures, such as nanosheet-based hollow spheres [11], 3D nanoflowers [12], self-assembled rings [13] and some other more complex structures [14–17], can improve its photocatalytic activity. In this paper, the strings of wheatear-shaped ZnO microstructures are assessed for their efficiency as photocatalysts. There are several techniques that can be used to synthesize ZnO nano- or microstructures. Chemical solution methods have become very popular in recent years owing to their low cost, simple process and capacity for large-scale production. ZnO with controllable morphologies have been produced through different hydrothermal processes with the assistance of specific surfactants and template agents [18–25].

The current team previously investigated the growth of 3D flower-like ZnO microstructures in zinc nitrate and high concentrations of sodium hydroxide solution [26]. The abundance of OH^- groups not only facilitated a rapid reaction but contributed to the oriented aggregating of ZnO primary particles considerably, which led to the final flower-like shape. Herein, a similar hydrothermal process is reported to prepare wheatear-shaped ZnO microstructures using zinc acetate and sodium hydroxide as raw materials. This approach is a pollution-free process and does not require any surfactant or template. The ultra-rapid growth of wheatear-shaped ZnO is also a highlight of this work.

2. Experimental

2.1 *Preparation and characterization*

All chemical reagents were of analytical grade and used without further purification. In a typical procedure, zinc acetate ($Zn(CH_3COO)_2 \cdot 2H_2O$) and sodium hydroxide (NaOH) were dissolved at room temperature in deionized water to obtain 1.0 and 4.0 mol l^{-1} standard solutions, respectively. About 30 ml of NaOH solution was added dropwise to 20 ml of $Zn(CH_3COO)_2$ solution with an additional 50 ml of deionized water under vigorous stirring at 3°C, resulting in a 100 ml clear solution containing $Zn(OH)_4^{2-}$ precursors ($[Zn^{2+}] = 0.2$ mol l^{-1}, $[OH^-] = 1.2$ mol l^{-1}). Then, the mixture was heated to 85°C and aged at constant temperature for 30 min. The white product wheatear-shaped ZnO was harvested after the reaction. The morphology and structure of the sample were characterized with a Hitachi S-4800 field-emission scanning electron microscopy (FESEM) system, a Bruker-AXS D8 ADVANCE X-ray diffractometer and a Quantachrome NOVA4000e surface area and pore size analyser.

2.2 *Growth process*

The growth of wheatear-shaped ZnO was studied by a time-dependent experiment. During the reaction, samples were collected from the mixture at regular time intervals. After filtration and washing, the solid phase was characterized by XRD and FESEM. The residual soluble zinc concentration was analysed by the EDTA chelate titration method.

2.3 *Photocatalytic experiments*

The photocatalytic experiments were conducted using methyl orange (MO) as a model dye under UV-light irradiation. A 250 W high-pressure Hg lamp ($\lambda_{max} = 365$ nm) was used for photodegradation test. An aqueous solution of MO (10 mg l^{-1}, 100 ml) and a photocatalyst (50 mg) were placed in a 200 ml beaker. The suspension was pretreated by ultrasound to disperse the catalyst, and then magnetically stirred in dark for 30 min to adsorption–desorption equilibrium. Then the suspension was placed under UV-light irradiation. A quantity of suspension was taken every 1 h to measure the MO degradation using a 752 N UV–vis spectrophotometer.

3. Results and discussion

3.1 *Characterization of as-prepared sample*

Wheatear-shaped ZnO microstructures were grown in an aqueous solution of zinc acetate and sodium hydroxide. The hydrothermal process was conducted at 85°C for 30 min. Scanning electron microscopy (SEM) images of the resulting crystals are shown in figure 1. The image with a low magnification (figure 1a) indicates that most particles are monodispersed wheatear-like structures. The length of the wheatear is about 5.8 μm and the section width is 1.2 μm. Figure 1b shows an enlarged SEM image of an individual particle. The wheatear-like particle consists of closely packed nanorods with average diameter of 100 nm. Each nanorod has a hexagonal prismatic structure. Most of them have a sharp pointed end extending outwards, and only a few have a hexagonal plane end extending outwards.

To obtain a further investigation on the porous material, the Brunauer–Emmett–Teller (BET) measurement was performed to show the characteristics of the pores. As shown in figure 2, the nitrogen adsorption–desorption isotherm is identified as a type IV curve accompanied by a type H3 hysteresis loop, revealing the existence of abundant mesoporous structures in the material [27]. However, due to the presence of large mesopores, the capillary condensation takes place at high relative pressures and adsorption saturation is not significantly visible. The corresponding Barrett–Joyner–Halenda (BJH) pore size distribution curve (inset in figure 2) indicates that most of the pores fall into the size ranging from 3.7 to 31.6 nm. The sharp peak at 3.7 nm may come from the tensile strength effect (TSE) and is not an indication of mesoporosity [28,29]. Further, the specific surface area of the wheatear-shaped ZnO is evaluated to be 9.617 $m^2\ g^{-1}$, which is larger than that of the commercial ZnO.

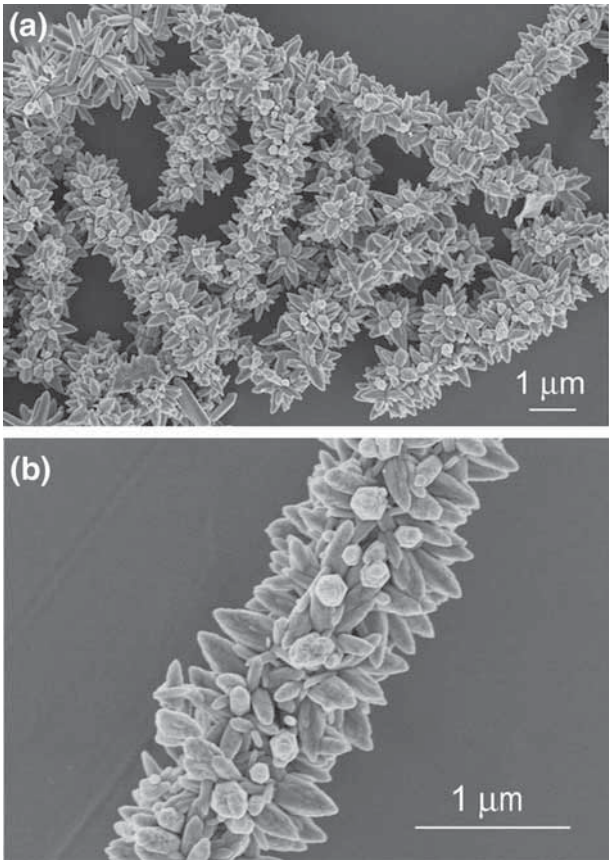

Figure 1. (**a**) Low-magnification SEM image showing the wheatear-shaped ZnO microstructures. (**b**) Enlarged SEM image showing the typical morphology of an individual particle.

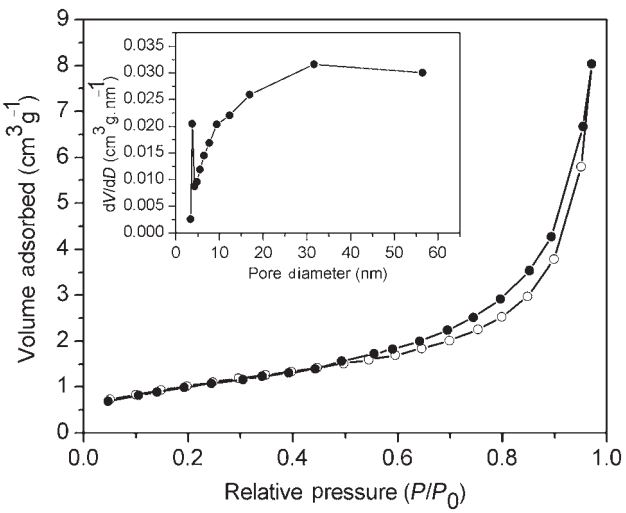

Figure 2. Nitrogen adsorption–desorption isotherm and BJH pore size distribution of wheatear-shaped ZnO samples.

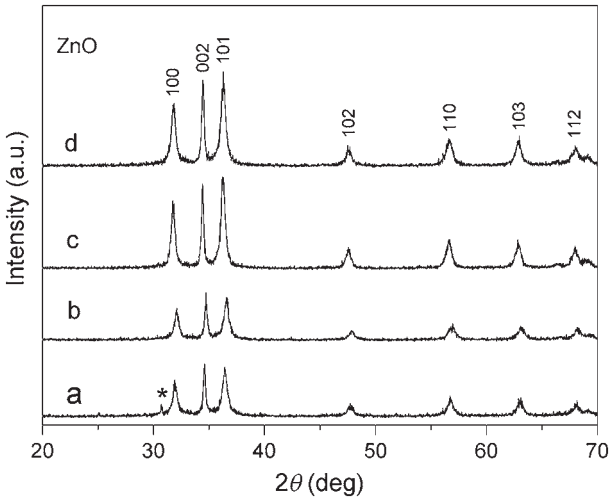

Figure 3. XRD patterns of samples at different growth times: (a) 0.5, (b) 1, (c) 2 and (d) 5 min.

3.2 *Growth mechanism of wheatear-shaped ZnO particles*

To uncover the mechanism of formation of the wheatear-shaped ZnO structures, a time-dependent experiment was conducted. We obviously observed that at the beginning of this process, a $Zn(OH)_2$ precipitate was obtained. As more of the NaOH solution was added, the $Zn(OH)_2$ precipitate dissolved to yield a homogenous aqueous solution containing $Zn(OH)_4^{2-}$ ions. Therefore, $Zn(OH)_4^{2-}$ is proposed to be the growth unit, which is directly incorporated into ZnO crystallites under given conditions. The growth process of ZnO can be formulated as follows:

$$Zn^{2+} + 2OH^- \rightarrow Zn(OH)_2 \downarrow \quad (1)$$

$$Zn(OH)_2 + 2OH^- \rightarrow Zn(OH)_4^{2-} \quad (2)$$

$$Zn(OH)_4^{2-} \rightarrow ZnO + 2H_2O + 2OH^- \quad (3)$$

The X-ray diffraction (XRD) patterns of the samples at the designated times are displayed in figure 3. Results showed that ZnO predominated in the phase at growth time of 0.5 min (curve a), except trace of impurities (indicated with an asterisk). At 1 min (curve b), the sample was identified as pure ZnO with a hexagonal wurtzite structure (JCPDS 36-1451). As growth continued (curves c and d), the intensity of the ZnO diffraction peaks increased significantly, indicating very good crystallization.

The morphologies of the samples at different stages of growth were identified in FESEM images (figure 4). When the reaction time was 0.5 min (figure 4a), the samples mainly contained flower-like structures with mean diameter of 500 nm, which could be identified as ZnO. When the reaction time was 1 min (figure 4b), short-wheatear-shaped ZnO was present in the samples, besides flower-like ZnO with an increased size of 820 nm. The length of the wheatear-shaped ZnO was about 2 μm and the section width was about 820 nm. When the reaction was prolonged to 2 min (figure 4c), wheatear-shaped ZnO predominated in the samples with almost the same size as the

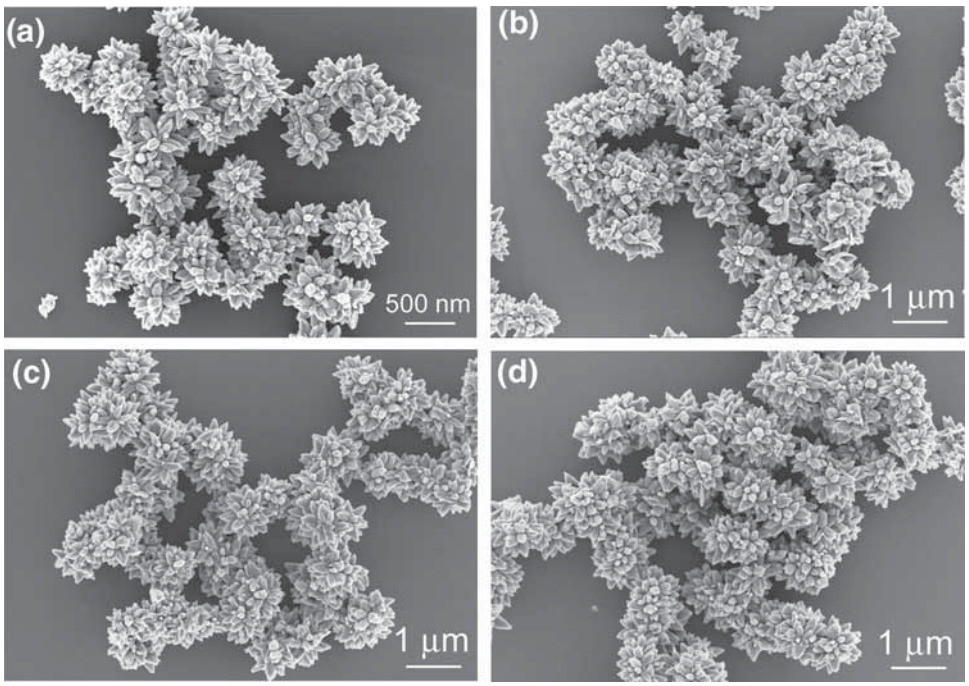

Figure 4. FESEM images of samples at different growth times: (**a**) 0.5, (**b**) 1, (**c**) 2 and (**d**) 5 min.

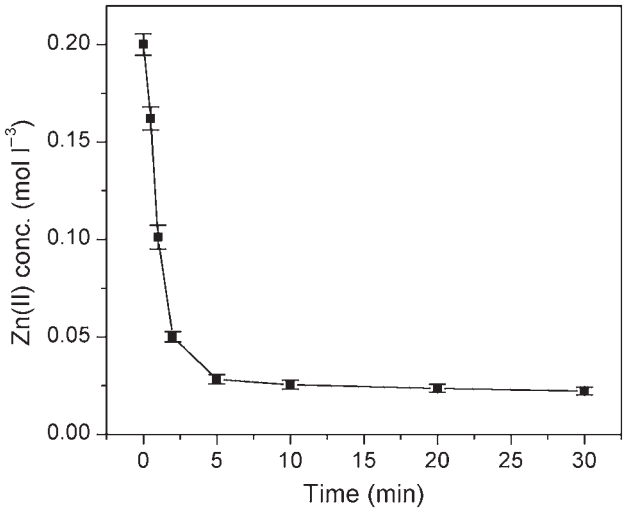

Figure 5. Soluble Zn(II) concentration *vs.* time in the mother liquid during reaction ($n = 3$, $\bar{x} \pm S$).

former. As reaction time continued to 5 min (figure 4d), the length and width of the wheatear-shaped structures increased.

The concentration of soluble Zn(II) remaining in the mother solution as a function of time was also determined (figure 5). In the first 5 min, Zn(II) concentration decreased in a linear manner, followed by a slow decline, indicating the production of a large number of crystal nuclei and the growth of the particles. The curve eventually plateaued after 5 min, indicating that dissolution–crystallization equilibrium of ZnO had been established.

The characterization of XRD, SEM and Zn(II) concentration over time shows that the growth of wheatear-shaped ZnO is a very rapid process. The nucleation and crystal growth were complete in almost 5 min. This is because the particularly high alkalinity of the solution provided abundant precursors of $Zn(OH)_4^{2-}$, which increased the reaction rate. thereupon, explosive nucleation of ZnO took place when the solution reached its critical temperature. A large number of primary bullet-shaped nuclei with structural polarity precipitated out of the solution in a short time. The tiny particles tended to aggragate due to their high surface energy and the frequent collisions between them. Because the high alkalinity of the solution provided a negative environment, most of the pointed ends (show positive) of the bullets were aligned towards the solution. Most of the plane ends (show negative) gathered around a few pointed ends. The secondary nuclei formed in a radiated mode, which looked like a flower. The tips of the flower petals were positive and the bottom of the petal junctions were strongly negative. The flower-like secondary nuclei continued to aggregate end to end, and the oriented growth continued. Eventually a string of wheatear-shaped ZnO structures formed. The multistep nucleation and oriented growth of wheatear-shaped ZnO structures are shown in a schematic illustration in figure 6.

3.3 *Photocatalytic activities*

It has been reported that the photocatalytic performance of ZnO can be affected by the morphology of the particles [30,31]. Because wheatear-shaped ZnO exhibits highly open

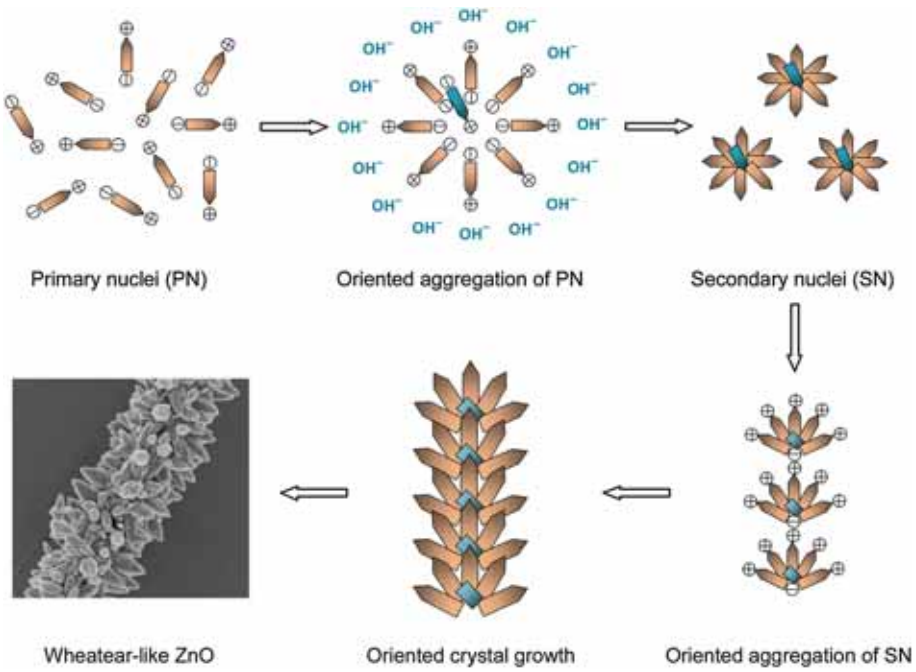

Figure 6. Schematic illustration of the formation process of wheatear-shaped ZnO microstructures.

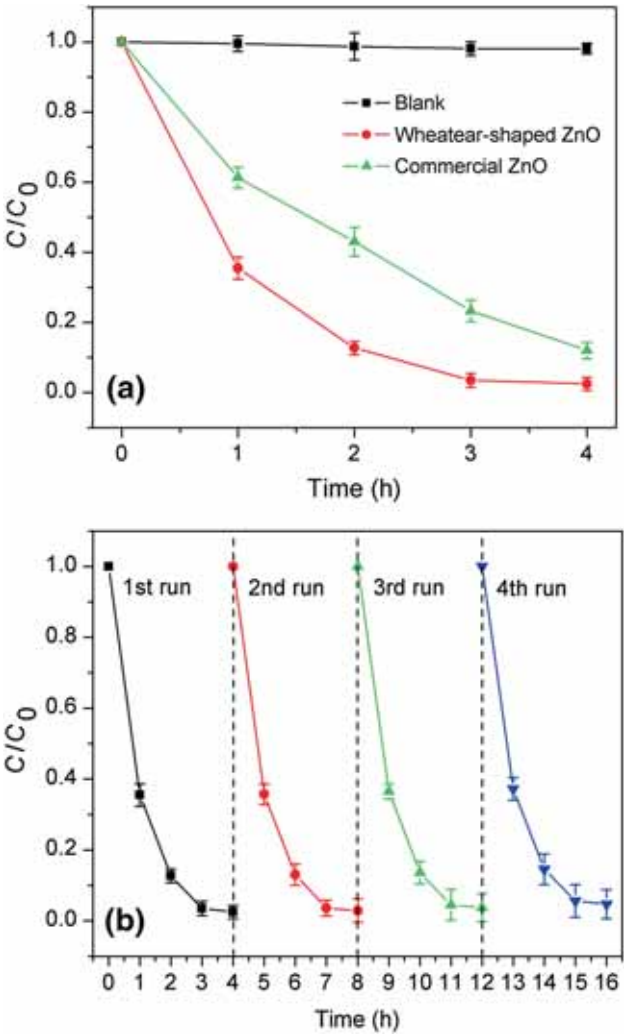

Figure 7. (**a**) Photodegradation curves of MO over ZnO and (**b**) photocatalytic recycling experiments using wheatear-shaped ZnO as the photocatalyst ($n = 3$, $\bar{x} \pm S$).

structures and maintains a large active surface area, it should be useful as an efficient photocatalyst for degradation of organic pollutants. In the current study, the photocatalytic performance of ZnO was evaluated using MO as a model dye under UV-light irradiation. As shown in figure 7a, there was almost no degradation of MO in the blank solution, which contained no photocatalyst. The samples of wheatear-shaped ZnO and commercial ZnO showed obvious activity for the degradation of MO. In addition, the wheatear-shaped ZnO exhibited better activity than that of commercial ZnO. The degradation efficiency of MO was 96.5% for wheatear-shaped ZnO after 3 h of UV-light irradiation, which was much higher than that for commercial ZnO (76.7%). To evaluate the stability of the wheatear-shaped ZnO catalyst, the cyclic experiments of the sample were carried out (figure 7b). After four cycles, there was no apparent decrease in the photodegradation efficiency, suggesting that the wheatear-shaped ZnO maintained relatively high photocatalytic activity.

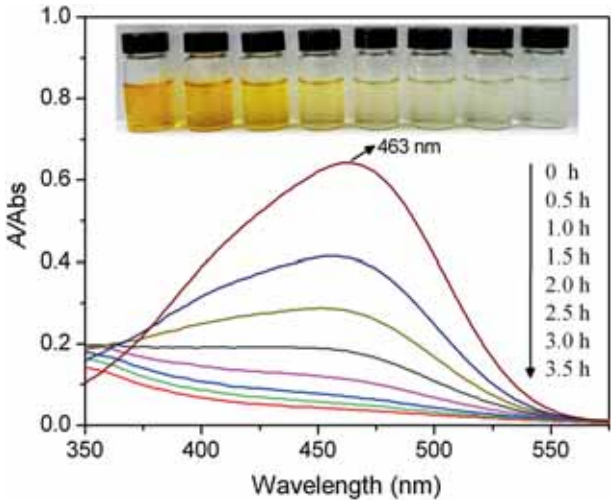

Figure 8. Absorption spectra of MO aqueous solution with wheatear-shaped ZnO for different durations. The inset shows the colour change of the MO solution from the initial time to 3.5 h.

Figure 8 shows temporal UV–vis absorption spectra of MO solution during the photocatalytic degradation in the presence of the wheatear-shaped ZnO. The maximum absorbance at 463 nm for MO molecules was observed to gradually decrease, and completely disappeared after irradiation for 3.5 h. Since no new absorption peak was observed, MO may be decomposed. Accordingly, the MO solution became almost colourless from bright orange as seen in the inset of figure 8. The results indicate that MO was mostly degraded within 3.5 h by the wheatear-shaped ZnO photocatalyst. As we know, the colour of the organic dye MO depends mainly on its chromophoric groups (–N=N–). When ZnO photocatalysts are irradiated by UV light, electrons (e^-) in the valence band (VB) can be excited to the conduction band (CB) with the simultaneous generation of holes (h^+) in the VB. Then, the holes (h^+_{VB}) will react with water or hydroxyl groups to generate $^\bullet$OH. The hydroxyl radicals $^\bullet$OH can destroy the azo groups in the MO molecules to accelerate the degradation of MO. In addition, the hierarchical wheatear-shaped ZnO may contribute to the superior photocatalytic performance. The open structures of ZnO samples enable better light harvesting and scattering; hence the utilization of the UV light, which is the 'direct stimulation' of the photocatalytic reactions, will be heightened [32]. On the other hand, the wheatear-shaped ZnO has mesoporous structure, which can improve its adsorption ability for organic pollutants, and is also convenient for the hydroxyl radicals OH and organic pollutants for diffusion and transport during the process of degradation.

4. Conclusions

In summary, novel wheatear-shaped ZnO structures were prepared *via* a simple one-step hydrothermal process. This approach is a rapid, environment-friendly process that does

not require any surfactants or templates. Due to the intrinsic polar structure of ZnO and the high alkalinity of the solution, OH^--driven oriented aggregation and multistep nucleation ultimately resulted in the formation of wheatear-shaped ZnO. The particles had complex structures and showed high photocatalytic activity towards MO under UV-light irradiation. This research may introduce new thinking into the growth of complex assembled materials in aqueous solutions.

Acknowledgements

This work was supported by the National Natural Science Foundation of China (21203052), and the Science Foundation of Hebei Normal University (L2015Z03). We also thank LetPub for its linguistic assistance during manuscript preparation.

References

[1] Edalati K, Shakiba A, Vahdati-Khaki J and Zebarjad S M 2016 *Mater. Res. Bull.* **74** 374
[2] Escobedo-Morales A, Téllez-Flores D, Peralta L R, Garcia-Serrano J, Herrera-González A M, Rubio-Rosas E *et al* 2015 *Mater. Chem. Phys.* **151** 282
[3] Sin J C, Lam S M, Lee K T and Mohamed A R 2015 *Mater. Lett.* **140** 51
[4] Yildirim O A, Liu Y and Petford-Long A K 2015 *J. Cryst. Growth* **430** 34
[5] Pimentel A, Nunes D, Duarte P, Rodrigues J, Costa F M, Monteiro T *et al* 2014 *J. Phys. Chem. C* **118** 14629
[6] Patil P, Gaikwad G, Patil D R and Naik J 2016 *Bull. Mater. Sci.* **39** 655
[7] Yang M, Sun K and Kotov N A 2010 *J. Am. Chem. Soc.* **132** 1860
[8] Hong Y, Tian C G, Jiang B J, Wu A P, Zhang Q, Tian G H *et al* 2013 *J. Mater. Chem. A* **1** 5700
[9] Cho S, Jang J W, Lee J S and Lee K H 2010 *Langmuir* **26** 14255
[10] Mujtaba J, Sun H Y, Fang F, Ahmad M and Zhu J 2015 *RSC Adv.* **5** 56232
[11] Khoa N T, Kim S W, Thuan D V, Yoo D H, Kim E J and Hahn S H 2014 *CrystEngComm.* **16** 1344
[12] Fan J C, Li T F and Heng H 2016 *Bull. Mater. Sci.* **39** 19
[13] Boppella R, Anjaneyulu K, Basak P and Manorama S V 2013 *J. Phys. Chem. C* **117** 4597
[14] Chang Z J 2011 *Chem. Commun.* **47** 4427
[15] Yang Y Q, Yang Y Q, Wu H X and Guo S W 2013 *CrystEngComm.* **15** 2608
[16] Wang J, Hou S C, Zhang L Z, Chen J C and Xiang L 2014 *CrystEngComm.* **16** 7115
[17] Ma W Q, Gu Z X, Nan H H, Geng B Y and Zhang X J 2015 *CrystEngComm.* **17** 1121
[18] Jung M H and Chu M J 2014 *J. Mater. Chem. C* **2** 6675
[19] Alenezi M R, Alshammari A S, Jayawardena K D G I, Beliatis M J, Henley S J and Silva S R P 2013 *J. Phys. Chem. C* **117** 17850
[20] Self K, Zhou H J, Greer H F, Tian Z R and Zhou W Z 2013 *Chem. Commun.* **49** 5411
[21] Liu Y X, Wang D S, Peng Q, Chu D R, Liu X W and Li Y D 2011 *Inorg. Chem.* **50** 5841
[22] Wang F, Qin X F, Zhu D D, Meng Y F, Yang L X and Ming Y F 2014 *Mater. Lett.* **117** 131
[23] Srinivasan P, Subramanian B, Djaoued Y, Robichaud J, Sharma T and Bruning R 2015 *Mater. Chem. Phys.* **155** 162
[24] Hirota Y, Elias M S, Dwijaya B, Uchida Y and Nishiyama N 2014 *Chem. Lett.* **43** 360
[25] Shi R X, Yang P, Song X L, Wang J P, Che Q D and Zhang A Y 2016 *Appl. Surf. Sci.* **366** 506
[26] Su Y M, Li J B, Luo Z Z, Lu B and Li P 2016 *RSC Adv.* **6** 7403
[27] Lu H B, Wang S M, Zhao L, Li J C, Dong B H and Xu Z X 2011 *J. Mater. Chem.* **21** 4228
[28] Singh S, Barick K C and Bahadur D 2013 *CrystEngComm.* **15** 4631
[29] Groen J C, Peffer L A A and Pérez-Ramírez J 2003 *Microporous Mesoporous Mater.* **60** 1
[30] Ali T T, Narasimharao K, Parkin I P, Carmalt C J, Sathasivam S, Basahel S N *et al* 2015 *New J. Chem.* **39** 321
[31] Prakash A and Bahadur D 2014 *Phys. Chem. Chem. Phys.* **16** 21429
[32] Liu Y S, Zhao N Q and Gao W 2013 *RSC Adv.* **3** 21666